

AtPIN4 Mediates Sink-Driven Auxin Gradients and Root Patterning in *Arabidopsis*

Jiří Friml,^{1,2,12} Eva Benková,^{1,3,11} Ikram Blilou,^{4,11} Justyna Wisniewska,^{1,5} Thorsten Hamann,⁶ Karin Ljung,⁷ Scott Woody,⁸ Goran Sandberg,⁷ Ben Scheres,⁴ Gerd Jürgens,⁶ and Klaus Palme^{1,9,10}

¹Max-Delbrück-Laboratorium
in der Max-Planck-Gesellschaft
Carl-von-Linné-Weg 10
50829 Köln
Germany

²Department of Biochemistry
Faculty of Science
Masaryk University
Kotlářská 2
611 37 Brno
Czech Republic

³Institute of Biophysics ASCR
Královopolská 135
612 65 Brno
Czech Republic

⁴Department of Molecular Cell Biology
Utrecht University
Padualaan 8
Utrecht, CH, 3584
The Netherlands

⁵Department of Biotechnology
Institute of General and Molecular Biology
87-100, Torun
Poland

⁶Zentrum für Molekularbiologie der Pflanzen
Universität Tübingen
Auf der Morgenstelle 3
72076 Tübingen
Germany

⁷Umeå Plant Science Center
Department of Forest Genetics
and Plant Physiology
The Swedish University of Agricultural Sciences
S 901 83 Umeå
Sweden

⁸Laboratory of Genetics
The University of Wisconsin
445 Henry Mall
Madison, Wisconsin 53706

⁹Institut für Biologie II – Zellbiologie
Universität Freiburg
Schänzlestrasse 1, 79104
Freiburg
Germany

Summary

In contrast to animals, little is known about pattern formation in plants. Physiological and genetic data

suggest the involvement of the phytohormone auxin in this process. Here, we characterize a novel member of the PIN family of putative auxin efflux carriers, *Arabidopsis* PIN4, that is localized in developing and mature root meristems. *Atpin4* mutants are defective in establishment and maintenance of endogenous auxin gradients, fail to canalize externally applied auxin, and display various patterning defects in both embryonic and seedling roots. We propose a role for AtPIN4 in generating a sink for auxin below the quiescent center of the root meristem that is essential for auxin distribution and patterning.

Introduction

Developing organisms are growing populations of cells that exchange information about their relative positions and respond accordingly, resulting in spatial patterns of differentiated cell types. The concept of positional information proposes concentration gradients of morphogens, which instruct cells within a field about their position (Wolpert, 1996). Experiments in animals identified several molecules with morphogen properties, such as Wingless, Hedgehog, and DPP in *Drosophila* imaginal discs (reviewed in Teleman et al., 2001), Squint in the Zebra fish embryo (Chen and Schier, 2001), or the Sonic Hedgehog in the chicken neural plate (Briscoe et al., 2001). By contrast, morphogen gradients have not been demonstrated in plants, although pattern formation occurs also beyond embryogenesis in specialized regions, the meristems, where cells continuously divide and differentiate according to their position (Steeves and Sussex, 1989). The plant hormone auxin (indole-3-acetic acid, IAA) has long been implicated in pattern formation based on indirect evidence from physiological and genetic studies (Sachs, 1985, 2000). Patterning defects have been reported for mutants perturbed in auxin signaling, such as *mp*, *ett*, *axr3*, as well as in embryos and seedling roots upon manipulation of auxin levels (reviewed in Berleth and Sachs, 2001). Recently, auxin levels in *Arabidopsis* roots have been inferred, at cellular resolution, from the expression of the *uidA* (GUS) reporter gene driven by the synthetic auxin-responsive promoter DR5. Elevated GUS activity levels, corresponding to an “auxin maximum,” were observed in the columella initials of the root cap, whereas auxin-induced changes of GUS activity correlated well with perturbations in patterning (Sabatini et al., 1999).

Conceptually, cellular auxin levels can be regulated by several processes such as production, degradation, (de)conjugation, or directional transport. Auxin is unique among plant hormones in being polarly transported through the vascular system away from the source tissues toward the root tip (Lomax et al., 1995). Auxin is then in part redirected back up to the distal elongation zone, thereby regulating root gravitropism (Rashotte et al., 2000). The concept of auxin transport, as described by the chemiosmotic hypothesis (Rubery and Sheldrake, 1974; Raven, 1975), proposes that transport is driven

¹⁰Correspondence: palme@mpiz-koeln.mpg.de

¹¹These authors contributed equally to this work.

¹² Present address: Zentrum für Molekularbiologie der Pflanzen, Universität Tübingen, Auf der Morgenstelle 3, 72076 Tübingen, Germany.

by a proton motive gradient and mediated by the action of influx and efflux carriers. The direction of auxin flux was proposed to be determined by asymmetric cellular localization of the efflux carrier. In search for these carriers, genetic approaches have been used to identify several auxin transport mutants in *Arabidopsis*, e.g., *aux1* (Bennett et al., 1996), *tir* (Ruegger et al., 1997), *rcn* (Garbers et al., 1996), and *pid* (Bennett et al., 1995). Another of these mutants, named *pin1* for its characteristic pin shape, showed a drastic reduction in basipetal auxin transport (Okada et al., 1991). The *AtPIN1* gene encodes a membrane protein with similarity to various transporter proteins from bacteria, consistent with a function of AtPIN1 as a component of the auxin efflux (Gälweiler et al., 1998). Even more strikingly, AtPIN1 was polarly localized to the basal ends of xylem parenchyma cells of *Arabidopsis* inflorescence axes in accordance with classical concepts. A homolog of *AtPIN1*, the *AtPIN2* gene, was shown to be involved in regulation of root gravitropism and auxin redistribution after gravity stimulation, presumably by facilitating upward auxin transport in the root epidermis (Chen et al., 1998; Luschnig et al., 1998; Müller et al., 1998). However, neither *Atpin1* and *Atpin2* nor mutants in the putative auxin influx carrier *AUX1* have revealed a role of auxin transport in regulating both auxin distribution and patterning.

Here, we describe the molecular analysis of the *AtPIN4* gene, a novel member of the *PIN* gene family. We demonstrate that AtPIN4 is expressed below the AtPIN1 domain in both developing and mature root meristems. We provide evidence that AtPIN4, but not AtPIN1, is essential for the correct establishment of an auxin gradient and is important for pattern formation in the root tip. Our results suggest a unique role for AtPIN4 in regulating both auxin homeostasis and patterning through sink-mediated auxin distribution in root tips.

Results

Isolation of the *AtPIN4* Gene

To identify additional members of the *Arabidopsis PIN* gene family, we screened the IGF bacterial artificial chromosome (IGF BAC) library with probes derived from conserved regions of *AtPIN1*. Eight positive BAC clones mapped to the same region near the top of chromosome 2 and contained the *AtPIN4* gene, which consists of six exons and five introns (Figure 1A). Using a gene-specific probe, we isolated a full-length cDNA. The cDNA is 2310 bp long and contains an open reading frame encoding a deduced protein of 616 amino acid residues with a predicted molecular mass of 66.7 kDa. A BLAST-based computer comparison revealed 65% and 64% identity with AtPIN1 and AtPIN2, respectively (Figure 1B). AtPIN4 has a three-domain topology characteristic of PIN proteins. Two N- and C-terminal hydrophobic regions each containing 4–6 putative transmembrane segments (amino acid residues 1–179 and 454–616) are linked by a hydrophilic region of 275 amino acids. In contrast to the highly conserved hydrophobic regions, this linker region is less conserved (Figure 1B).

To investigate the function of the *AtPIN4* gene, we isolated three mutant alleles termed *Atpin4-1*, *-2*, and *-3* and constructed antisense (*CaMV35S::asAtPIN4*)

transgenic plants (Figure 1A; for details see Experimental Procedures). Northern blot analysis using an *AtPIN4*-specific probe identified a transcript of ~2 kb in roots, seedlings, siliques, stems, leaves, and cotyledons (Figure 1C). No *AtPIN4*-specific signal was observed in seedlings of *Atpin4-1*, *-2*, and *-3* homozygous mutants, suggesting that these mutants were null (Figure 1D).

AtPIN4 Is Localized in Root Meristem Precursor Cells of the Embryo

To determine the localization of AtPIN4, we performed whole-mount in situ immunolocalization experiments using an AtPIN4-specific antiserum. No AtPIN4 signals were detected in early-globular embryos (Figure 2A). In late-globular embryos, strong AtPIN4 staining (indicated by red) was observed along the surface of the hypophysis and at the basal end of the adjacent suspensor cell (Figure 2B). During the triangular and subsequent developmental stages, suspensor staining gradually disappeared and additional signals appeared around the provascular cells with a maximum of the staining at the basal end (Figures 2C and 2D). In addition, the endodermis initials stained prominently at the heart stage (Figure 2E). The weak staining occasionally observed in epidermis of the apical embryo part (Figures 2A–2E) corresponds to a crossreaction with another AtPIN protein, since it can be observed also in *Atpin4* mutant embryos (data not shown). In situ hybridization with an *AtPIN4*-specific antisense riboprobe labeled the basal end of the embryo, suggesting that spatial accumulation of AtPIN4 protein was determined by transcriptional control (Figure 2F, compare with Figure 2E). This was confirmed by the expression pattern of a transcriptional fusion of the *AtPIN4* promoter with the GUS reporter gene that labeled the basal region corresponding to the quiescent center precursors and surrounding cells (Figure 2G). We also identified a marker line, originally designated *LENNY*, with an insertion of Ds-GUS (Sundaresan et al., 1995) downstream of *AtPIN4* promoter that exhibited a staining pattern identical to the *AtPIN4* expression pattern (Figure 2H).

Disruption of *AtPIN4* Affects DR5-Driven Reporter Expression in Embryos

We studied auxin accumulation in wild-type and *Atpin4* mutant, using a synthetic auxin-responsive promoter (*DR5rev*) fused to the reporter gene *PEH A* (Dotson et al., 1996). A similar construct (*DR5::GUS*) has been used to visualize auxin accumulation at cellular resolution in *Arabidopsis* roots (Sabatini et al., 1999). Wild-type embryos expressed PEH A very weakly in the basal part of the embryo from the early-heart stage on (Figures 3A–3E). The staining intensity was increased in late-heart and torpedo-stage embryos and the signal remained restricted to the basal part, with a maximum of PEH A activity in columella precursor cells (Figures 3D and 3E). In contrast, *Atpin4-1* (34 of 52), *Atpin4-2* (24 of 50), and *Atpin4-3* (68 of 81) mutant embryos showed a significantly different PEH A activity pattern (Figures 3F–3J). Strong staining was observed in all subepidermal cells of globular proembryos (Figure 3F). At triangular and heart stages, the domain of PEH A activity was located mostly in the presumptive vascular tissue and

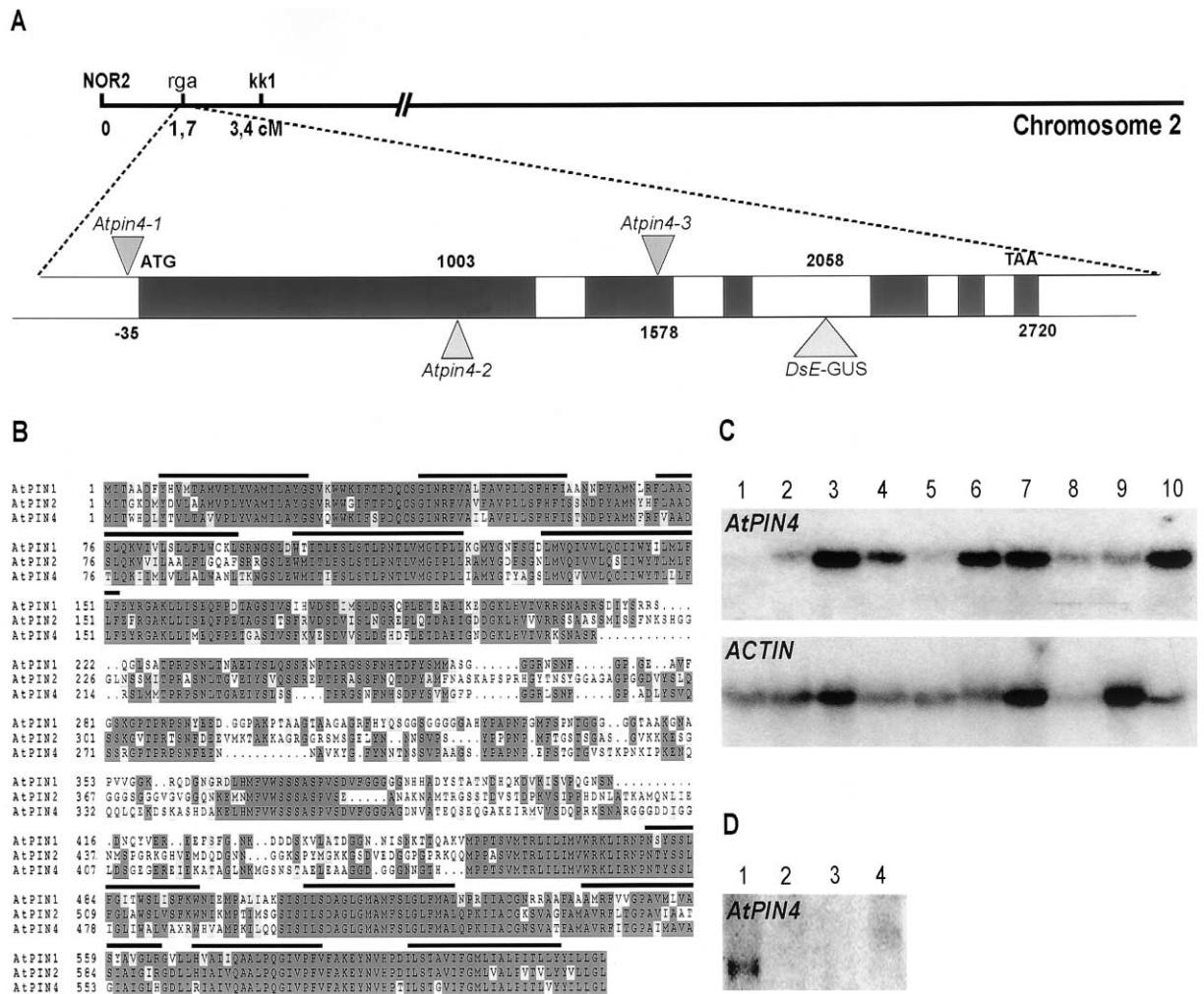


Figure 1. Genomic Organization and Expression of the *AtPIN4* Gene

(A) Structure of the *AtPIN4* genomic region. Adjacent markers and genetic distances are shown on the chromosomal map. Below, an enlarged view of the *AtPIN4* gene is presented with exons (black boxes) and introns (empty boxes). *En-1* transposon insertion sites and the *DsE* insertion site are marked by gray triangles with nucleotide position from ATG indicated.

(B) Comparison of AtPIN1, 2, and 4 protein sequences. The amino acid number is shown on the left. Identical amino acids are indicated as black boxes and gaps as dots. Bars above the sequence blocks denote transmembrane domain segments as predicted by the Kyte and Doolittle method.

(C) Northern blot analysis of *AtPIN4* mRNA in different tissues. Total RNA extracted from different *Arabidopsis thaliana* tissues and hybridized to an *AtPIN4* probe. (1) Wild-type suspension culture cells; (2) roots from *Arabidopsis* plants grown in liquid culture; (3) cauline leaves; (4) inflorescence; (5) siliques; (6) seedlings grown on MS agar for 6 days; (7) rosette leaves; (8) roots; (9) flowers; (10) cotyledons. All blots were rehybridized to a constitutively expressed *ACTIN* gene for control for loading.

(D) Northern blot analysis of *AtPIN4* mRNA from *Atpin4* mutant seedlings. Seedlings with genotype (1) *Atpin4-1* het; (2) *Atpin4-1*; (3) *Atpin4-2*; (4) *Atpin4-3*.

was thus enlarged and shifted upward relative to the position in corresponding wild-type embryos (Figures 3G–3I, compare with Figures 3B–3D). At the torpedo stage, *Atpin4* mutant embryos displayed more restricted staining which, in contrast to wild-type, had its maximum in basal provascular cells (Figure 3J, compare with Figure 3E). Thus, lack of *AtPIN4* function raised auxin levels as indicated by increased PEH A reporter activity. Moreover, the basally localized auxin response maximum of wild-type embryos was shifted apically in *Atpin4* embryos. Together, these changes suggest that AtPIN4 is involved in both regulating auxin levels and proper

positioning of the auxin response maximum in *Arabidopsis* embryogenesis.

Disruption of *AtPIN4* Affects Patterning in the Developing Root Meristem

To determine functional requirement of *AtPIN4* during embryogenesis, we compared the development of wild-type and *Atpin4* mutant embryos. No difference was observed prior to the globular stage ($n = 91$), at which stage cell divisions started to deviate from the stereotypic pattern of wild-type in the region of the future root meristem (Figure 4). In wild-type, the hypophysis divides

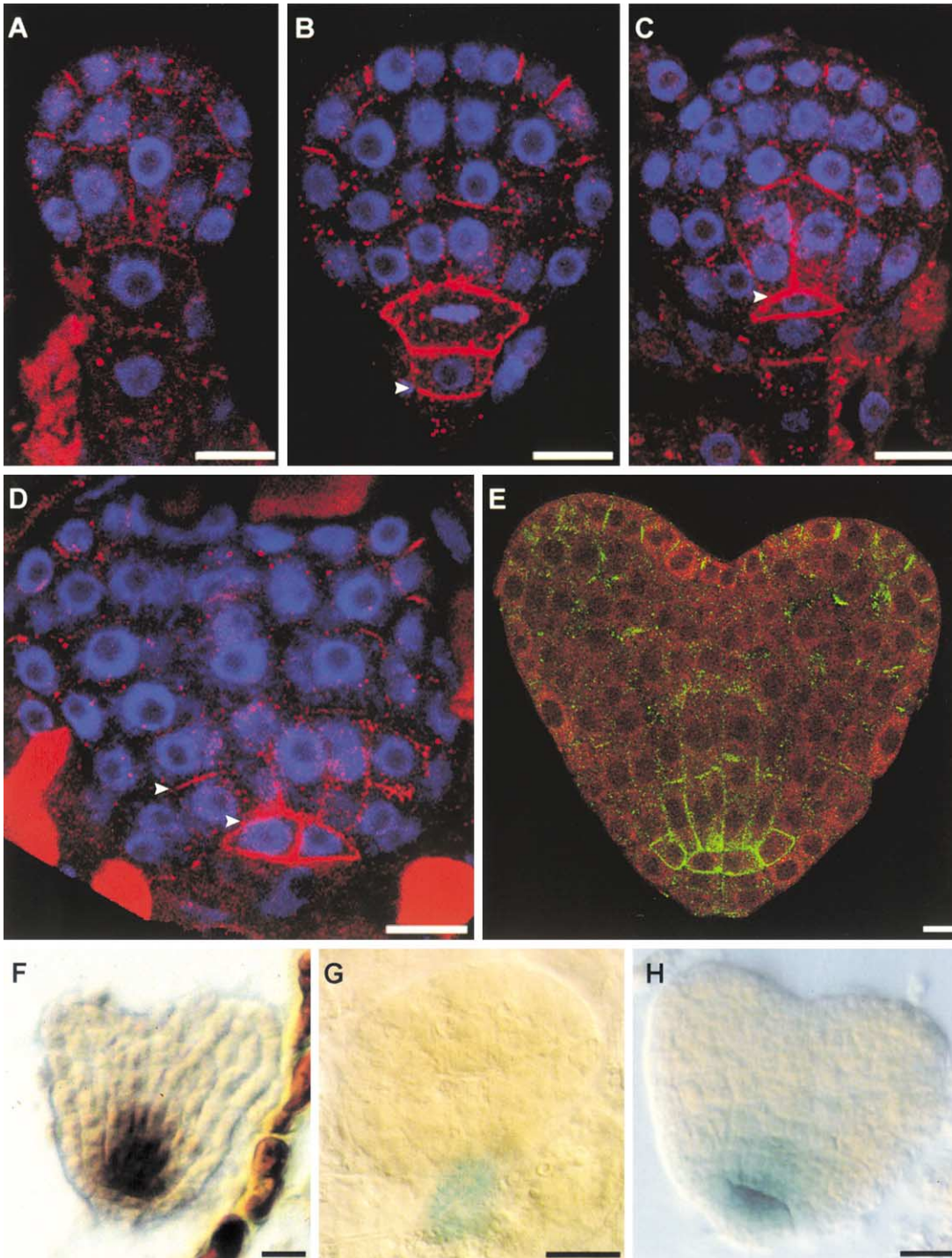


Figure 2. Expression and Localization of the AtPIN4 Protein during Embryogenesis

(A) Early globular stage. No AtPIN4 protein was found.

(B) Globular stage prior to hypophysis division: the hypophysis cell boundary is marked for AtPIN4. AtPIN4 is also found in the neighboring suspensor cell at the basal cell boundary.

(C) Late globular stage. The hypophysis cell has divided. The lens-shaped and provascular initial cells are stained for presence of AtPIN4. Weaker AtPIN4 signal marks the basal side of basal cell.

(D) Triangular stage: the lens-shaped cell has divided and AtPIN4 is distributed equally at the boundaries of QC cells. The provascular initials show label at their basal sides.

(E) Heart stage: additional AtPIN4 signal appears in the endodermis and provascular initials with the majority of signal at the basal boundaries.

(F) Heart stage: *AtPIN4* mRNA localization by in situ hybridization in the root meristem region.

(G) Globular stage: GUS staining of transgenic plants carrying *AtPIN4::GUS* construct in the root meristem region.

(H) Heart stage: GUS staining in the root meristem region of enhancer trap line *LENNY*.

AtPIN4 protein localization is indicated by red (CY3-conjugated secondary antibody; [A], [B], [C], and [D]) or by green (FITC-conjugated secondary antibody; [E]). The nuclei were stained with DAPI (A–D), indicated with blue. Basal staining indicated by arrowheads. Scale bars, 10 μ m.

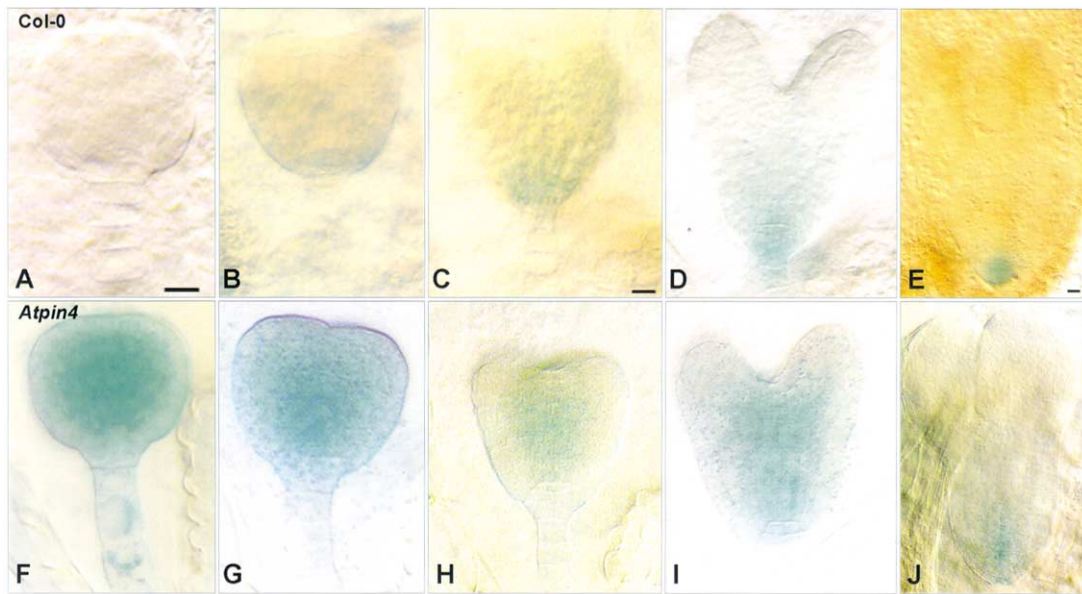


Figure 3. DR5 Auxin Response Reporter in Wild-Type and *Atpin4* Mutant Embryos

(A–E) During wild-type embryogenesis, expression is first detected in early heart stage (C) at the basal embryo end. During later stages, the maximum of *DR5rev::PEH A* expression is localized in QC cells and in the cells below.

(F–J) In *Atpin4* null mutant embryos, the *DR5rev::PEH A* expression can be detected at the midglobular stage in the inner proembryo cells (F). During the progression to the torpedo stage, the PEH A activity remains increased in comparison to wild-type and is often mislocalized in the area above the QC cells (G–J). The PEH A activity is indicated by blue. Scale bars, 10 μ M.

asymmetrically to give an upper lens-shaped cell and a larger lower cell (Figure 4A). Whereas the former gives rise to the quiescent center of the root meristem, the latter produces the single layer of columella initials. In wild-type embryos, the division of the basal cell occurred only rarely before the triangular stage (4/149) (Figure 4A) and the division of the lens-shaped cell never took place before the heart stage (0/149) (Figure 4B). In *Atpin4* mutant embryos, however, these cells divided prematurely at the globular stage (Figure 4C). These premature cell divisions occurred frequently in mutant embryos for each of the three alleles (*Atpin4-1*: 18/119; *Atpin4-2*: 20/122; *Atpin4-3*: 29/133) and in *AtPIN4* antisense embryos (12/48). Later in embryogenesis, the normally nondividing quiescent center (QC) cells showed divisions, and columella precursor cells underwent supernumerary divisions (Figure 4F, compare with Figure 4E). In addition, abnormal planes of cell division were observed, e.g., in columella precursors (Figure 4F). Furthermore, periclinal divisions of the uppermost suspensor cell (Figure 4D) occurred in *Atpin4* mutant (16/83) and *AtPIN4* antisense (12/56) heart-stage embryos, whereas wild-type suspensor cells divided anticlinally before mitotic quiescence at this stage. The aberrant cell divisions correlated with an altered expression pattern of the QC-specific marker, QC25, described previously for the postembryonic root (Sabatini et al., 1999). We determined that wild-type embryos expressed QC25 exclusively in QC cells already at the heart stage (Figure 6N). In contrast, *Atpin4* embryos expressed QC25 in a much broader domain (Figure 6O). Thus, a molecular marker confirms morphological observations, suggesting cell fate changes of the meristem cells in developing root.

***AtPIN1* and *AtPIN4* Are Expressed in Partially Overlapping Regions of the Seedling Root**

Transcripts and proteins of *AtPIN1* and *AtPIN4* were localized in primary roots by whole-mount in situ hybridization and immunolocalization, respectively (Figure 5). *AtPIN1* mRNA accumulated in the vascular cylinder but was absent from epidermis, cortex, quiescent center (QC), and root cap (Figure 5A). No staining was detected with the *AtPIN1* sense control (Figure 5A, inset). *AtPIN1* protein accumulated in the same cells as the mRNA, and was detected mostly at their lower (basal) ends (Figure 5B). In addition, a weaker *AtPIN1* signal was also observed in endodermis tissue. *AtPIN4* mRNA was localized in the QC and the surrounding cells of the root meristem (Figure 5C), whereas no signal was observed with the sense probe (Figure 5C, inset). *AtPIN4* protein was detected in the same tissues, including the QC, the surrounding initials, and their daughter cells (Figure 5D). Higher magnification revealed both polar and nonpolar localization of *AtPIN4* (Figure 5E). Whereas columella initials and columella cells displayed a nonpolar localization of *AtPIN4*, the cells of the proximal meristem, including endodermis, cortex, vascular initials, and their daughter cells, had *AtPIN4* localized at their lower (basal) ends. The QC cells had most *AtPIN4* label basally, although this polarity was less pronounced (Figure 5E). No label was observed in the roots of *Atpin4* null mutants and *AtPIN4* antisense seedlings (Figure 5F), although at higher antibody concentrations, crossreaction with another PIN protein was observed (data not shown). The spatial distributions of *AtPIN1* and *AtPIN4* partially overlapped in vascular initials and their derivatives (compare Figures 5B and 5D). The distinct patterns of

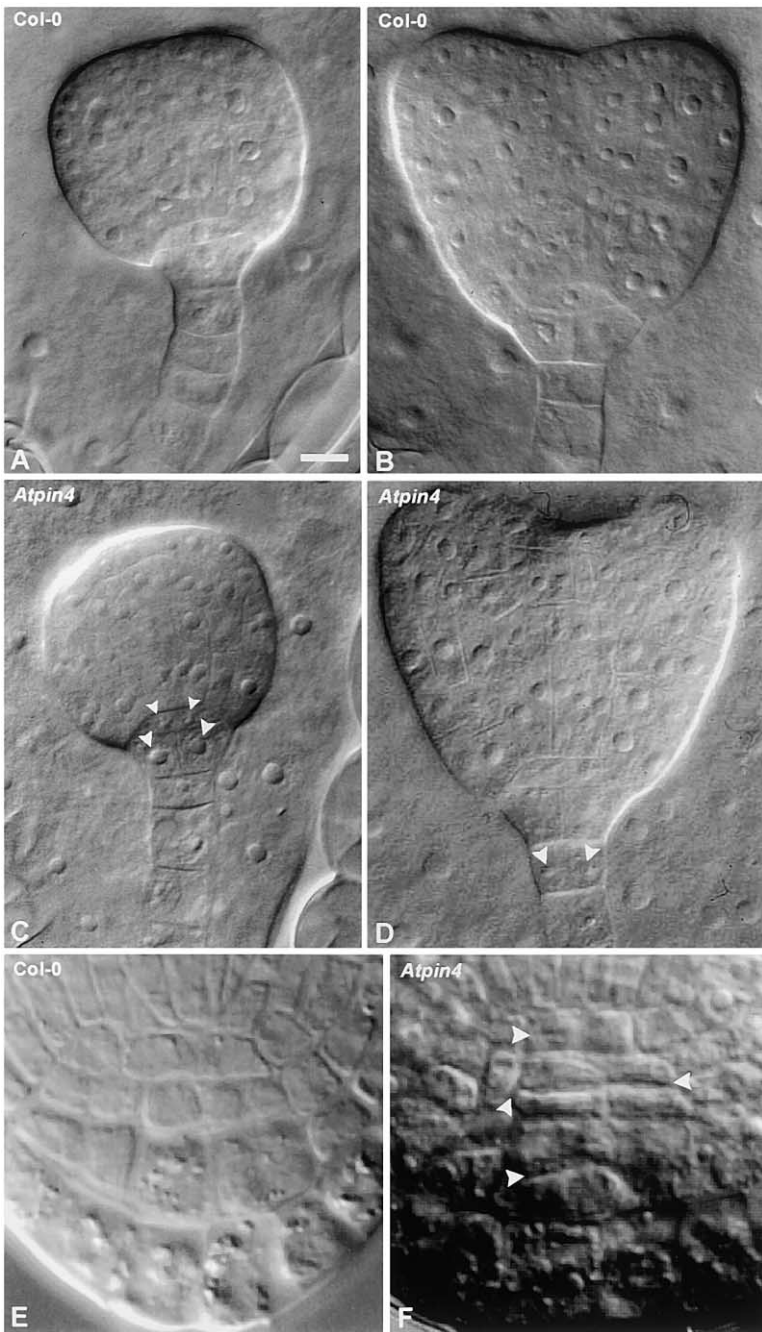


Figure 4. Embryonic Cell Division Aberrations in *Atpin4* Mutants

(A) Wild-type globular embryo: the lens-shaped and basal cells have not yet divided. (B) Wild-type heart stage embryo: the lens-shaped cell is still undivided, the basal cell has already divided, and no periclinal divisions appear in the suspensor. (C) *Atpin4* mutant globular embryo: both lens-shaped and basal cells have divided prematurely. (D) *Atpin4* mutant heart stage embryo: aberrant periclinal division in suspensor cell. (E) Wild-type mature embryo: QC, surrounding initials, and two columella precursors are visible. (F) *Atpin4* type bent-cotyledon embryo: aberrant QC divisions and additional tier of columella initial precursors as well as irregular divisions in columella precursors are visible. Arrowheads indicate the position of nuclei (C and D) or cell walls (F) of aberrantly divided cells in *Atpin4* mutant embryos. Scale bars, 10 μ M.

AtPIN1 and AtPIN4 localization suggest a basally directed auxin flow in roots through the vascular cylinder toward the central root meristem, where it focuses into columella initials and columella.

Atpin1 Mutant Roots Display No Defects

AtPIN1 plays a role in long-distance basipetal auxin transport within the inflorescence axis (Gälweiler et al., 1998). Our immunolocalization studies suggest a comparable role in mediating auxin flow to the root meristem region. However, we did not observe any obvious differences in root growth or gravitropic responsiveness of *Atpin1* mutant seedlings, as compared to wild-type (n =

286). Nor did we find any aberrations in root patterning between *Atpin1* (Col-0 ecotype) and Col-0 wild-type roots (n = 286). These results were in contrast to previously reported patterning defects and changes in *DR5::GUS* expression in the *Atpin1* mutant (Sabatini et al., 1999). Detailed inspection of the progeny from the original cross between *DR5::GUS* (Col-0) and *Atpin1* (Enkheim) revealed that the reported aberrations appear to involve an Enkheim-specific modifier. Moreover, the analysis of another cross between *Atpin1* (Col-0) and *DR5rev::GUS* (Col-0) did not reveal the previously reported abnormalities (data not shown). Taken together, these data show that *Atpin1* mutation may only in certain

circumstances affect root development and may reflect functional redundancy between different members of the *AtPIN* gene family.

Disruption of *AtPIN4* Affects DR5-Driven Reporter Expression and Auxin Levels in Roots

To determine the physiological consequences of *AtPIN4* disruption, we examined the auxin-responsive expression of *DR5rev::PEH A* in roots of transgenic wild-type and *Atpin4* mutant seedlings. Wild-type roots displayed *PEH A* reporter activity in the initials and the first cell layer of the columella (43 of 43) (Figure 6A). Treatment with 1–5 μ M NPA, which impairs auxin transport, increased *PEH A* reporter activity, and also expanded its expression domain (39 of 41) (Figure 6B). *Atpin4* mutant roots resembled NPA-treated roots in their pattern of *PEH A* expression (*Atpin4-1*: 49 of 71; *Atpin4-2*: 24 of 36; and *Atpin4-3*: 46 of 62). The *PEH A* activity was increased compared to wild-type and its maximum was centered on cells that corresponded to the QC and vascular initials in wild-type (Figure 6C). These results suggested that in the *Atpin4* root meristem, auxin levels were elevated, and the maximum was shifted to cells that display polar localization of *AtPIN4* protein in wild-type (compare Figure 6C with Figure 5E).

To directly correlate the *PEH A* signal with auxin levels, we measured the auxin content in root segments by mass spectrometry. We observed significantly elevated free IAA levels ($P < 0.005$) in the first mm of root tips in *Atpin4* mutant seedlings, as compared to wild-type (Figure 7A). By contrast, no significant differences in free IAA levels were observed in the second mm of root tips, which is farther away from the root meristem (data not shown). Thus, direct measurement of free IAA content confirmed the DR5-based observations, supporting the notion that *AtPIN4* is involved in the regulation of auxin levels and gradients in the root meristem.

AtPIN4 Is Involved in Maintenance of Auxin Gradient and Auxin Canalization in Roots

To test how roots regulate auxin levels, we challenged wild-type and *Atpin4* seedlings by incubation with 10 μ M IAA and subsequently analyzed *DR5rev::PEH A* expression. In wild-type roots, the maximum of *PEH A* activity was restricted to a few cells, including the columella initials (42 of 43) (Figure 6D). This pattern was qualitatively similar to untreated roots, implying that the roots have homeostatic mechanisms that can handle the elevated IAA levels and maintain endogenous auxin gradients. In contrast, wild-type roots exposed to IAA in the presence of the auxin transport inhibitor NPA exhibited a general increase of *PEH A* activity that, in addition, was expanded across the whole root tip (38 of 41) (Figure 6E). This result suggests that polar auxin transport is the major component for auxin canalization and maintenance of IAA gradients in the root tip. *Atpin4* mutant roots treated with exogenous IAA resembled NPA-treated wild-type roots, displaying highly increased levels of *PEH A* activity across the whole root tip (*Atpin4-1*: 23 of 33; *Atpin4-2*: 22 of 35; and *Atpin4-3*: 18 of 29). (Figure 6F). In addition, the maximum of *PEH A* staining was shifted to a zone apical to the QC, with elevated levels also in the endodermis (Figure 6F). These results

suggest that *Atpin4* roots are not able to maintain endogenous IAA gradients, fail to mediate flow of exogenously applied IAA to the columella region, and to neutralize it.

To confirm our DR5-based observations and to gain insights into the dynamics of IAA turnover, a study was performed with mass spectrometry to measure the relative turnover of IAA after its exogenous application (Figure 7B). The amount of IAA taken up by the root tips measured immediately after a feeding period of 30 min was significantly lower ($P < 0.05$) in *Atpin4* mutant than in wild-type roots. This reduced ability of *Atpin4* roots to accumulate exogenous IAA is in accordance with our notion that *Atpin4* mutants display impaired IAA transport, which probably prevents feeding of the columella region. We also observed that the decrease of free IAA content within the first three hours in *Atpin4* roots was significantly smaller ($P < 0.005$) than in wild-type roots, confirming our DR5-based observations. This observation suggests a reduced capacity of *Atpin4* roots to downregulate the IAA pool in this tissue, probably due to a defect in canalization IAA fluxes (Figure 7B).

Disruption of *AtPIN4* Affects Root Meristem Patterning

To determine functional requirement of *AtPIN4* in post-embryonic development, we compared the growth and pattern of wild-type and *Atpin4* mutant roots. By comparing root meristems between wild-type and *Atpin4* mutants (Figures 6G–6K), we observed several distinct aberrations in cell patterns of four-day-old seedling roots (Figure 6H, compare with Figure 6G). Abnormal roots were observed in 95%–97% of the seedling progeny of *Atpin4* homozygous mutant plants, regardless of the allele examined (*Atpin4-1*: 40 of 42; *Atpin4-2*: 55 of 57; *Atpin4-3*: 47 of 48). Identical pattern aberrations occurred in 38 of 38 *AtPIN4* antisense seedlings (Figure 6I). The well-defined QC of mitotically quiescent cells was replaced by cells that divided in irregular planes (Figure 6H, arrowheads). In addition, the mutant displayed two, instead of one, tiers of columella initials (Figure 6H, arrows) and supernumerary cells in the differentiated columella layers with often aberrant shapes (Figures 6H and 6S). Endodermis cells of *Atpin4* mutant roots also behaved abnormally, undergoing periclinal divisions (Figure 6H, inset, arrow). As seedling development progressed, aberrations became more pronounced, and the root meristem often completely lost its regular pattern (Figures 6J and 6K). The columella formed up to eight additional layers of root cap cells (*Atpin4*: 34 of 92; *AtPIN4* antisense: 59 of 112; Figures 6I and 6J) and massive periclinal divisions in the proximal root meristem led to a characteristic swelling of the root tip (*Atpin4*: 19 of 92; *AtPIN4* antisense: 23 of 112; Figure 6K). The many features of *Atpin4* root meristem phenotype, including QC divisions, extra columella cell columns, endodermis periclinal divisions, and extra root cap and swelling, were mimicked by growing wild-type seedling on 1 μ M NPA (Figure 6B, data not shown), further supporting a role of *AtPIN4* in auxin efflux.

To gain further insight into the changes of cell identities in *Atpin4* mutant roots, we analyzed expression patterns of cell-type-specific markers. The expression domains

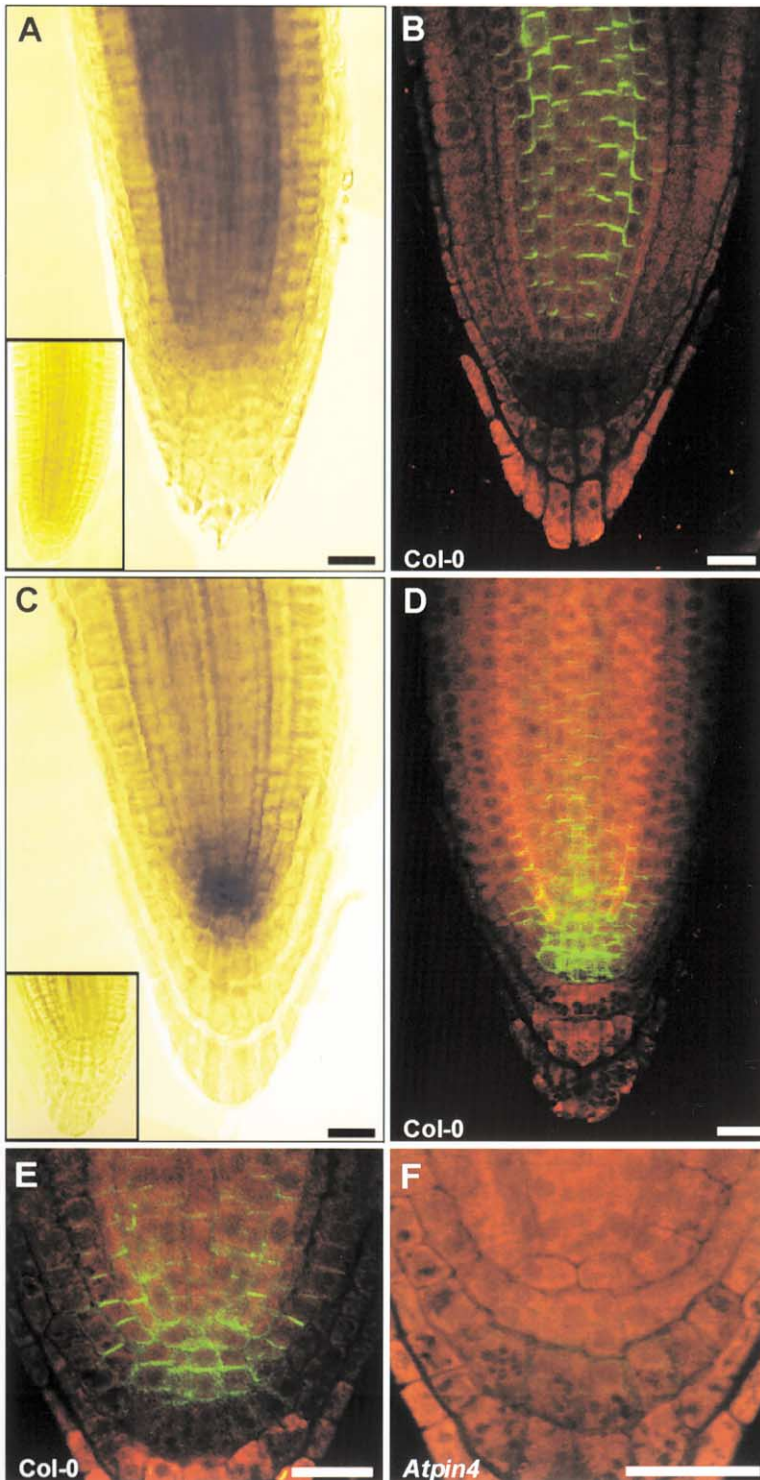


Figure 5. Expression and Localization of AtPIN1 and AtPIN4 in Wild-Type and Mutant Roots

(A) Whole-mount in situ hybridization reveals *AtPIN1* mRNA in the central part of root. No *AtPIN1* mRNA is found in root cap, cortex, or epidermis. No staining is detected in a control experiment using *AtPIN1* sense probe (inset).

(B) Whole-mount in situ immunolocalization of the AtPIN1 protein. The AtPIN1 signal is found in the plasma membrane of stele cells, while weaker signal is also detected in endodermis cells. The AtPIN1 protein is predominantly located at the basal side of cells. No signal is detected in the QC.

(C) Whole-mount in situ hybridization shows the presence of *AtPIN4* mRNA in QC and all surrounding initials and daughter cells. No staining is detected in control experiment using *AtPIN4* sense probe (inset).

(D) Whole-mount in situ immunolocalization of the AtPIN4 protein. The AtPIN4 label was found at the boundaries of QC cells and surrounding cells.

(E) Detail of AtPIN4 polar localization in the central root meristem.

(F) No AtPIN4 protein was found in *Atpin4* homozygous plants.

AtPIN1 and *AtPIN4* mRNA is indicated by dark brown. AtPIN1 and AtPIN4 proteins were detected by FITC-conjugated secondary antibody indicated by green. The autofluorescence of root tissue is indicated by red. Scale bars, 20 μ m.

of QC cell fate marker QC25 (Figures 6L–6O) and QC/columella marker COL148 (Figures 6P and 6Q) were expanded, suggesting that root meristem initials and their daughter cells displayed some features of QC cells. Conversely, cells at the QC position in *Atpin4* mutant seedlings display much weaker and frequently (12/13), no detectable expression of *pSCR::GFP*, in contrast to

wild-type (1/34) QC cells (Figure 6S, compare with Figure 6R). This observation was further confirmed by Northern blot analysis with an *SCR*-specific probe (data not shown). In addition, endodermal cells originating from periclinal divisions displayed weak or no expression of *pSCR::GFP*, confirming changes in cell behavior (Figures 6R and 6S, insets). The columella differentiation

defect in *Atpin4* mutant seedlings was reflected in the abnormal expression of the columella initial marker J2341 in the supernumerary tier of columella initials (Figure 6U, arrows; compare with Figure 6T). In addition, the cells located at the position of wild-type QC also expressed the marker J2341 (Figure 6U, arrowhead; compare with Figure 6T), suggesting that these cells adopted at least some features of columella initials. The staining pattern of five different cell type markers, in conjunction with changes in cell morphology and behavior, strongly suggest changes in cell fate, with QC and surrounding cells probably adopting mixed cell fates. Taken together, loss of *AtPIN4* function affects rate and orientation of cell divisions, polar expansion, and cell fates within the root meristem.

Discussion

AtPIN4 Is a Novel Regulator of Auxin Efflux

The *AtPIN4* gene encodes a member of the PIN family of putative auxin efflux carriers (Friml, 2000) that all share limited structural similarity with transport proteins of the major facilitator group (Marger and Saier, 1993). Although auxin transport has not been biochemically demonstrated for any PIN protein, our findings suggest that *AtPIN4* functions either as an auxin carrier or a regulator of auxin transport. As shown previously for other PIN proteins, *AtPIN4* is polarly localized, and the mutant phenotype can be mimicked by chemical inhibition of auxin efflux in wild-type plants. In addition, we observed defects in *Atpin4* mutants outside of the *AtPIN4* expression domain, suggesting non cell autonomous action of *AtPIN4* consistent with a role in long-range signaling. We also detected a shift in auxin-responsive gene expression, which spatially correlated with the loss of *AtPIN4* expression. Taken together, our observations support the notion that *AtPIN4* represents an important regulatory component of polar auxin transport, possibly an auxin efflux carrier.

Localized *AtPIN4* Expression Is Required for Graded Auxin Distribution

Direct auxin measurements have demonstrated auxin gradients in scots pine (Uggla et al., 1996). In the *Arabidopsis* root tip, locally elevated auxin levels (auxin maximum) have been inferred for the columella initials and the columella region (Sabatini et al., 1999). *AtPIN4* is expressed in the quiescent center and surrounding cells of developing and mature root meristems, and the protein is localized toward this auxin maximum. In *Atpin4* mutants as well as in wild-type roots treated with auxin-transport inhibitors, the auxin distribution is altered with the maximum shifted from the columella initials upward to a broader and more diffuse domain encompassing the QC and vascular initials. Concomitantly, auxin response reporter expression was increased, which was directly correlated with elevated auxin levels in root tips, as measured by mass spectroscopy. Comparable changes were observed in mutant embryos, suggesting that *AtPIN4* is involved not only in maintaining, but also in establishing an auxin gradient with a basally located auxin maximum. How this gradient is mechanistically established is not known. In animal systems, diffusion, cell proliferation,

and planar transcytosis have been discussed as ways to establish morphogen gradient (Teleman et al., 2001). The active cell-to-cell transport of auxin mediated by auxin carrier proteins shares some similarities with the transcytosis model involving cycles of endo- and exocytosis, as proposed for Wingless gradient formation in *Drosophila* (Bejsovec and Wieschaus, 1995). In support of this analogy, *AtPIN1* has recently been demonstrated to cycle between the plasma membrane and endosomal compartments (Geldner et al., 2001).

AtPIN4 Links Auxin Transport and Patterning

Although auxin has been occasionally discussed as a plant morphogen, experimental examination of such a model was hampered by the lack of specific mutants and tools to visualize auxin levels at cellular resolution (Berleth and Sachs, 2001). This situation has changed with the availability of the cellular markers for auxin response and mutants that are defective in auxin gradients. Whereas previous studies attempting to link auxin and patterning relied on exogenous manipulation of auxin homeostasis or auxin transport (Hadfi et al., 1998, Kerk and Feldman, 1994, Sabatini et al., 1999), *Atpin4* mutants display specific corresponding changes in auxin distribution and pattern aberrations, including changes in rate and plane of cell divisions, cell fate determination, and polar cell expansion. Most strikingly, our data suggest that novel cell fates inferred from molecular marker analysis correlate spatially with changes in auxin distribution. Cells positioned at and above the shifted auxin maximum acquire features of columella-initial and QC fates, respectively. Moreover, the domains of novel cell fate are both enlarged and partially overlapping, which corresponds with the broadened and fuzzy auxin maximum in the *Atpin4* mutant. Taken together, these results strongly suggest that a graded distribution of auxin is instructive for cell fate acquisition, thus supporting a role for auxin as a morphogen.

AtPIN4-Dependent Auxin Gradients are Sink-Driven

Our data suggest that a graded distribution of auxin with a maximum basal to the QC of the root correlates with correct patterning. The extension of this maximum to the root base after loss of *AtPIN4*, which is polarly localized toward the columella, suggest that auxin is supplied by the more basal tissues and transported into the maximum region in an *AtPIN4*-dependent fashion. Thus, the auxin maximum in the root is established against the slope of the gradient away from the source of auxin production.

The continuous auxin supply through the stele to the maximum region raises the question of what happens to auxin there. *Atpin4* mutant plants, as well as plants with chemically inhibited auxin transport, are defective in local auxin inactivation, implying that auxin is down-regulated in root tip. However, other members of the PIN family (e.g., *AtPIN2* and *AtPIN3*), together with the auxin permease AUX1, apparently facilitate lateral and basipetal rerouting of a portion of auxin from columella cells through root cap, epidermal, and cortical cell layers back up to the distal elongation zone thereby regulating gravitropism (Friml et al., 2002; Rashotte et al., 2000, 2001; Swarup et al., 2001). Available evidence suggests

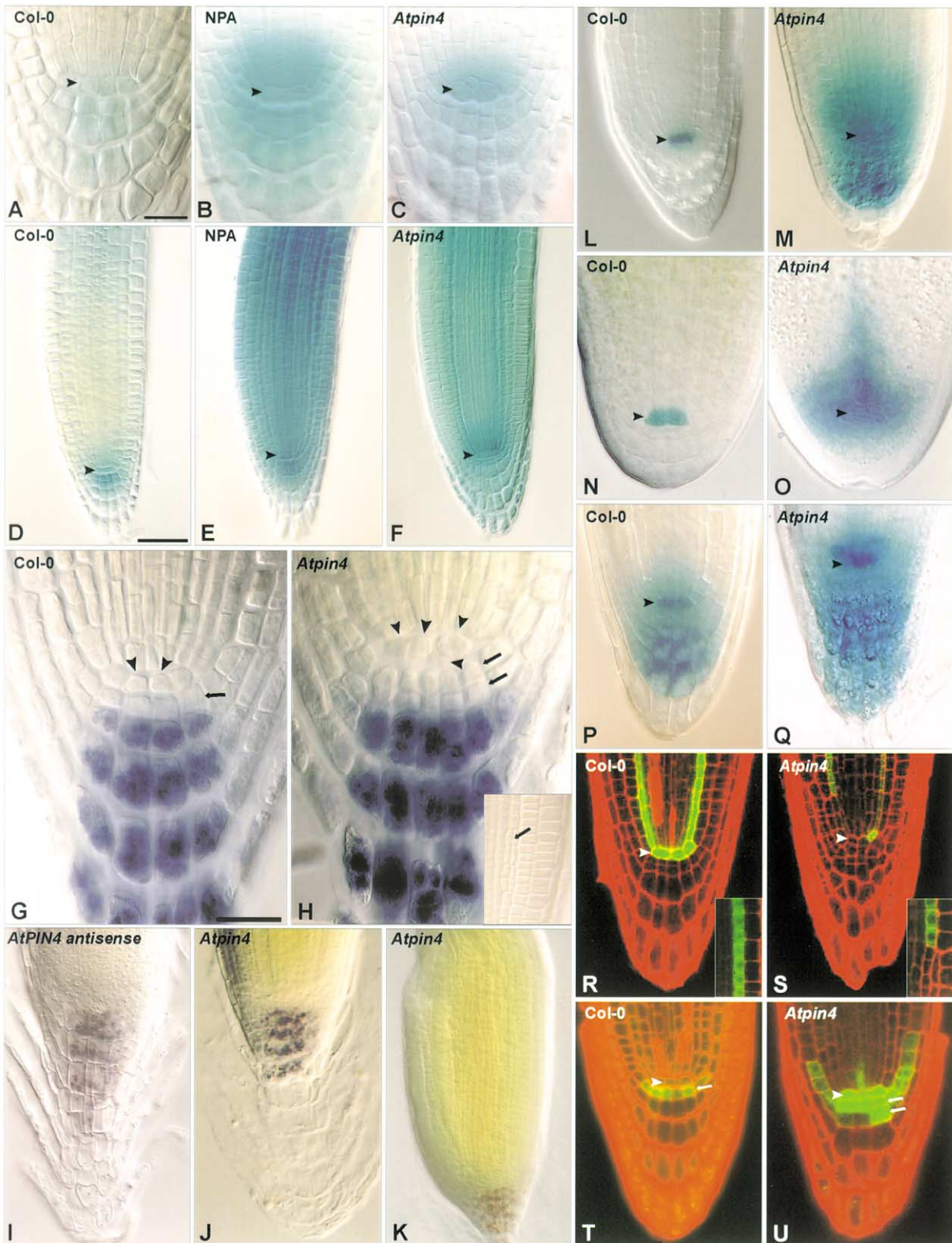


Figure 6. Meristem Pattern, DR5 Auxin Response Reporter, and Cell Marker Expression in Wild-Type and *Atpin4* Mutant Roots
 (A–C) *DR5rev::PEH A* expression in root meristem of wild-type (A and B) and *Atpin4* mutant (C) transgenic plants. The maximum of *DR5rev::PEH A* expression in wild-type is detected in columella initials and first columella tier (A). In contrast, in NPA-treated plants (B) and in *Atpin4* mutants (C), the *DR5rev::PEH A* expression maximum is shifted into QC cells and vascular initials, and the overall PEH A activity in root tip is elevated.
 (D–F) *DR5rev::PEH A* expression in root meristem of wild-type (D and E) and *Atpin4* mutant (F) plants after four hours of IAA treatment. In

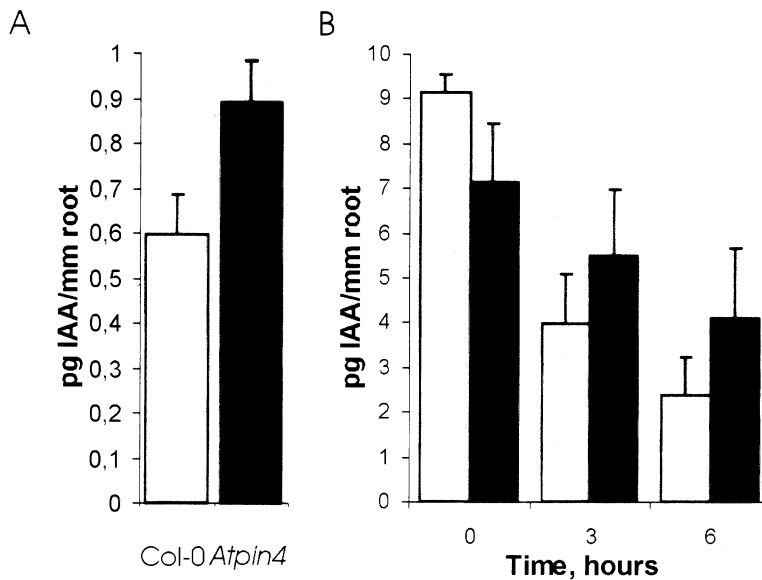


Figure 7. IAA Content and IAA Turnover in Wild-Type and *Atpin4* Mutant Roots

(A) IAA content in the bottom millimeter (mm) of wild-type and *Atpin4* mutant roots. Presented data represent mean and standard deviations of six individual measurements (two experiments, each performed in triplicate).
(B) IAA turnover in the bottom mm of wild-type and *Atpin4* mutant roots after IAA feeding. Four to five samples were analyzed. Error bars indicate standard deviations.

that the region of the auxin maximum below the QC acts as an *AtPIN4*-dependent sink for auxin. We propose that this basal sink controls the auxin distribution and thereby patterning, since chemical or genetic interference with the sink abolishes this gradient. By contrast, the auxin distribution is maintained in the presence of additional external auxin sources. Our analyses of the *Atpin4* embryo phenotype and *AtPIN4* embryo localization pattern suggest a similar mechanism for controlling auxin levels and patterning in embryogenesis.

Our model of a sink-driven morphogenetic auxin gradient in the *Arabidopsis* root tip contrasts with the well-established morphogen gradients in animals that are source driven (reviewed in Teleman et al., 2001), such as the anterior-posterior gradient of Bicoid in the *Drosophila* preblastoderm embryo (Driever and Nüsslein-Volhard, 1988) or the spreading of the DPP gradient from the anterior-posterior compartment boundary in the

Drosophila wing imaginal discs (Basler and Struhl, 1994). Nonetheless, the principle of cell fate determination based on the relative concentrations of a morphogen at specific positions along the gradient may apply in plants as well as in animals.

Experimental Procedures

Materials and Growth Conditions

The *AtPIN4* gene was identified in the IGF BAC genomic library (<http://www.mpimp-golm.mpg.de/mpi-mp-map/>) with an *AtPIN1* probe (nucleotides 1–385; accession number AF089084; Gälweiler et al., 1998). The full-length *AtPIN4* cDNA was isolated from cDNA libraries prepared from seedlings, leaves, and whole plant tissues. The primer pair 5'-CTCAAATGCCACTGTCTTCTCACT-3' and 5'-ATCTTCTTCTCACCTCCACTCT-3' was used to amplify the *AtPIN4* genomic sequence (accession number AF087016). *AtPIN4* antisense plants were generated using a construct spanning 157–822 nucleotides of *AtPIN4* cDNA in antisense orientation under the control of the CaMV35S promoter. The construct for monitoring of endoge-

wild-type plants (D), the *DR5rev::PEH A* expression pattern does not qualitatively differ from the untreated roots (A). Simultaneous IAA and NPA application in wild-type (E) results in dramatic increase of *DR5rev::PEH A* expression in the whole root. This effect is phenocopied by IAA application in *Atpin4* mutants (F) resulting in a dramatic increase of *DR5rev::PEH A* expression. The ectopic increase of *DR5rev::PEH A* expression was detected in endodermis cells and the expression maximum in vascular initial cells.

(G and H) Lugol-stained root tips of 4-day-old wild-type (G) and *Atpin4* mutant (H) seedlings. In *Atpin4*, cells at the position of the wild-type QC show irregular cell division planes. Additionally, two tiers of columella initials and five columns of columella cells are found instead of a single columella tier and four columella cell columns in wild-type. The inset in (H) indicates the periclinal divisions (denoted by black arrow) in endodermis cells of *Atpin4* mutant root. Arrowheads indicate wild-type QC cells and cells in corresponding area in *Atpin4* mutant. Arrows indicate position of columella initial tiers.

(I–K) 10-day-old lugol-stained roots of transgenic plants carrying the *CaMV35S::αAtPIN4* antisense construct (I) or *Atpin4* mutants (J and K). Additional layers of root cap (I and J) and massive swelling of the root meristem (K) are visible.

(L and M) GUS staining of the QC-specific promoter trap QC25 in 3-day-old wild-type roots (L) was detected exclusively in QC. In *Atpin4* mutant (M), GUS staining is elevated with expression detected additionally in surrounding initial and daughter cells.

(N and O) GUS staining of the QC-specific promoter trap QC25 in torpedo-stage wild-type embryos (N) was detected exclusively in QC. In *Atpin4* mutant (O), GUS staining was increased with additional expression in surrounding initials and daughter cell precursors.

(P and Q) GUS staining of the QC and columella-specific promoter trap COL148 in 3-day-old wild-type roots (P) was detected in QC and columella. In *Atpin4* mutant (Q), GUS staining appears additionally in QC surrounding initials.

(R and S) *pSCR::GFP* expression in 3-day-old wild-type roots (R) was detected in endodermis and QC. In *Atpin4* mutant (S), *pSCR::GFP* expression is lower, with no expression detected in QC.

(T and U) Expression of J2341, a GFP-based columella initials marker in 3-day-old wild-type roots (T) was detected in columella initials. In *Atpin4* mutant (U), J2341 expression marks two columella initial tiers and is additionally detected at the position of the wild-type QC.

Lugol staining is indicated by dark purple, GUS activity by blue, and GFP fluorescence by green, respectively. Arrowheads indicate position of wild-type QC and the corresponding area in *Atpin4* mutant. Arrows indicate position of columella initial tiers.

nous auxin levels *DR5::GUS* was described by Ulmasov et al. (1997). *DR5rev::PEHA* consists of nine repeats of the DR5 element (TGCTCTC) fused in inverse orientation to the minimal CaMV35S promoter and the phosphonate monoester hydrolase, *PEH A* (Dotson et al., 1996) gene. The *AtPin4::GUS* construct was generated by fusion of a PCR-amplified fragment (nucleotides -1764 to -1 upstream of ATG and the GUS gene). The homozygous *Atpin4-1*, -2, and -3 mutant lines were identified by reverse genetic screening of an *En-1* transposon mutagenized collection of *A. thaliana* (Col-0) as described (Müller et al., 1998). Six *En-1* insertions were identified and flanking regions sequenced. Three introns-located insertions were not further analyzed. The other insertions, termed *Atpint4-1*, -2, and -3 were located 35 nucleotides upstream of the start codon, and in the first and second exons at positions 1003 and 1578, respectively. The following probes and primers were used: nucleotides 1429–2012 and nucleotides 679–1149 of the *AtPIN4* cDNA, 5'-CTCAATGCCACTGTCTTCTCACT-3', and 5'-ATCTTCTTCTCACCTTCCACTCT-3'. The *LENNY* line contains the Ds-GUS transposon inserted within the third intron of the *AtPIN4* gene at position 2058. Marker lines J2341, COL148, *pSCR::GFP*, and QC25 were previously described (Sabatini et al., 1999).

Expression Analysis and Immunolocalization

Histochemical staining for GUS and PEH A activity was performed using modified indigenic method with 5-bromo-4-chloro-3-indoxyl β -D glucuronide (X-Gluc, *Sigma*) or 5-bromo-4-chloro-3-indoxyl phosphonate (XPP, Research Organics) as substrates (Dotson et al., 1996; Sabatini et al., 1999). For all comparisons between wild-type, NPA treated wild-type, and *Atpin4* lines, identical staining conditions were used. In the case that a different transgenic insertion was used, at least four independent lines (>40 roots each) were analyzed. Northern blot analysis and whole-mount in situ hybridization experiments were performed as described (Müller et al., 1998) with probes corresponding to a region of *AtPIN4* (nucleotides 679–1149). *AtPIN4*-specific antibodies were generated using a recombinant protein corresponding to amino acids 243 to 400 of *AtPIN4* as described (Gälweiler et al., 1998). Immunolocalizations in roots and embryos were performed as described (Steinmann et al., 1999; Müller et al., 1998). Affinity-purified primary anti-*AtPIN1* (Gälweiler et al., 1998) and anti-*AtPIN4* antibodies were diluted 1:150 and 1:200, respectively. The secondary antibodies, FITC-conjugated and CY3-conjugated anti-rabbit antibody (Dianova) were diluted 1:200 or 1:600, respectively. Solutions during the whole-mount in situ hybridization and immunolocalization procedures were changed using a pipetting robot (Insitu Pro, Intavis).

Growth Conditions and Microscopy

Plant growth conditions were as previously described (Müller et al., 1998). Exogenous auxin application was performed by incubation of 4-day-old seedlings in 0.5 \times MS liquid medium supplemented by 10–25 μ M IAA and/or 25 μ M NPA for 0.5 to 6 hr. Starch granules in the central root cap were visualized by lugol staining and for histological analysis of embryos; dissected ovules were fixed and cleared as described (Sabatini et al., 1999). Both embryos and roots were viewed with Nomarski optics using a Leica DMRB microscope equipped with a video camera (Hitachi, HV-C20A). Fluorescent samples were inspected by confocal laser scanning microscopy as described (Müller et al., 1998). Images were processed using Adobe Photoshop 4.0 (Adobe Systems, Inc.) and final composition of figures was performed with CorelDRAW 7 (Corel Corporation).

Analysis of IAA Contents and Turnover Rates

For each sample, 1 mm root segments from 50 seedlings were collected and pooled. For turnover studies, seedlings were incubated in medium containing 10 μ M IAA for 30 min, thoroughly washed, and transferred to MS medium for the rest of the incubation period. The samples were extracted, purified, and analyzed by combined GC-SRM-MS (gas chromatography-selected reaction monitoring-mass spectrometry) as described (Edlund et al., 1995). Calculation of isotopic dilution factors was based on the addition of 100 pg $^{13}\text{C}_6$ -IAA to each sample. The significance of reported differences in IAA content and IAA turnover was interpreted from the T values.

Acknowledgments

We thank Petra Tänzler, Michaela Lehnen, and Thomas Steinmann for technical help. We acknowledge the Arabidopsis Biological Resource Center (Columbus, OH) and Thomas Altman for providing material. We also gratefully acknowledge the ADIS service group for DNA sequencing and ZIGIA (Center for Functional Genomics in Arabidopsis) for the *En* lines. We are grateful to our colleagues, particularly Leo Gälweiler, Niko Geldner, Matthias Godde, and Kathrin Schrick for critical reading of the manuscript. This work was supported by a fellowship of the Deutscher Akademischer Austauschdienst (J.F.), the Deutsche Forschungsgemeinschaft (Schwerpunktprogramm Phytohormone), the European Communities Biotechnology Programs, the Fonds der Chemischen Industrie, and the INCO-Copernicus Program.

Received: October 29, 2001

Revised: January 22, 2002

References

- Basler, K., and Struhl, G. (1994). Compartment boundaries and the control of *Drosophila* limb pattern by hedgehog protein. *Nature* 368, 208–214.
- Bejsovec, A., and Wieschaus, E. (1995). Signalling activities of the *Drosophila* wingless gene are separately mutable and appear to be transduced at the cell surface. *Genetics* 139, 309–320.
- Bennett, S.R.M., Alvarez, J., Bossinger, G., and Smyth, D.R. (1995). Morphogenesis in pinoid mutants of *Arabidopsis thaliana*. *Plant J.* 8, 505–520.
- Bennett, M.J., Marchant, A., Green, H.G., May, S.T., Ward, S.P., Millner, P.A., Walker, A.R., Schulz, B., and Feldmann, K.A. (1996). *Arabidopsis* AUX1 gene: a permease-like regulator of root gravitropism. *Science* 273, 948–950.
- Berleth, T., and Sachs, T. (2001). Plant morphogenesis: long-distance coordination and local patterning. *Curr. Opin. Plant Biol.* 4, 57–62.
- Briscoe, J., Chen, Y., Jessell, T.M., and Struhl, G. (2001). A hedgehog-insensitive form of patched provides evidence for direct long-range morphogen activity of sonic hedgehog in the neural tube. *Mol. Cell* 7, 1279–1291.
- Chen, Y., and Schier, A.F. (2001). The zebrafish nodal signal squint functions as a morphogen. *Nature* 411, 607–610.
- Chen, R., Hilson, P., Sedbrook, J., Rosen, E., Caspar, T., and Masson, P. (1998). The *Arabidopsis thaliana* *AGRAVITROPIC 1* gene encodes a component of the polar-auxin-transport efflux carrier. *Proc. Natl. Acad. Sci. USA* 95, 15112–15117.
- Dotson, S.B., Lanahan, M.B., Smith, A.G., and Kishore, G.M. (1996). A phosphonate monoester hydrolase from *Burkholderia caryophylli* PG2982 is useful as a conditional lethal gene in plants. *Plant J.* 10, 383–392.
- Driever, W., and Nüsslein-Volhard, C. (1988). The bicoid protein determines position in the *Drosophila* embryo in a concentration-dependent manner. *Cell* 54, 95–104.
- Edlund, A., Eklöf, S., Sundberg, B., Moritz, T., and Sandberg, G. (1995). A microscale technique for gas chromatography–mass spectrometry measurements of picogram amounts of indole-3-acetic acid in plant tissues. *Plant Physiol.* 108, 1043–1047.
- Friml, J. (2000). Isolation and characterization of novel *AtPIN* genes from *Arabidopsis thaliana* L. PhD thesis, University of Cologne, Köln, Germany.
- Friml, J., Wisniewska, J., Benkova, E., Mendgen, K., and Palme, K. (2002). Lateral relocation of auxin efflux regulator PIN3 mediates tropism in *Arabidopsis*. *Nature* 415, 806–809.
- Gälweiler, L., Guan, C., Müller, A., Wisman, E., Mendgen, K., Yephremov, A., and Palme, K. (1998). Regulation of polar auxin transport by *AtPIN1* in *Arabidopsis* vascular tissue. *Science* 282, 2226–2230.
- Garbers, C., Delong, A., Deruere, J., Bernasconi, P., and Soll, D.

- (1996). A mutation in protein phosphatase 2A regulatory subunit A affects auxin transport in *Arabidopsis*. *EMBO J.* **15**, 2115–2124.
- Geldner, N., Friml, J., Stierhoff, Y., Jürgens, G., and Palme, K. (2001). Polar auxin transport inhibitors block PIN1 cycling and vesicle trafficking. *Nature* **413**, 425–428.
- Hadfi, K., Speth, V., and Neuhaus, G. (1998). Auxin-induced developmental patterns in *Brassica juncea* embryos. *Development* **125**, 879–887.
- Kerk, N., and Feldman, L. (1994). The quiescent centre in roots of maize: initiation, maintenance, and role in organization of the root apical meristem. *Protoplasma* **183**, 100–106.
- Lomax, T.L., Muday, G.K., and Rubery, P.H. (1995). Auxin transport. In *Plant Hormones: Physiology, Biochemistry and Molecular Biology*, 2nd edition, P.J. Davies, ed. (Norwell, MA: Kluwer Academic Publishers) pp.509–530.
- Luschnig, C., Gaxiola, R.A., Grisafi, P., and Fink, G.R. (1998). EIR1, a root-specific protein involved in auxin transport, is required for gravitropism in *Arabidopsis thaliana*. *Genes Dev.* **12**, 2175–2187.
- Marger, M.D., and Saier, M.H., Jr. (1993). A major superfamily of transmembrane facilitators that catalyze uniport, symport, and antiport. *Trends Biochem. Sci.* **18**, 13–20.
- Müller, A., Guan, C., Gälweiler, L., Taenzler, P., Huijser, P., Marchant, A., Parry, G., Bennett, M., Wisman, E., and Palme, K. (1998). AtPIN2 defines a locus of *Arabidopsis* for root gravitropism control. *EMBO J.* **17**, 6903–6911.
- Okada, K., Ueda, J., Komaki, M.K., Bell, C.J., and Shimura, Y. (1991). Requirement of the auxin polar transport system in early stages of *Arabidopsis* floral bud formation. *Plant Cell* **3**, 677–684.
- Rashotte, A.M., Brady, S.R., Reed, R.C., Ante, S.J., and Muday, G.K. (2000). Basipetal auxin transport is required for gravitropism in roots of *Arabidopsis*. *Plant Physiol.* **122**, 481–490.
- Rashotte, A.M., DeLong, A., and Muday, G.K. (2001). Genetic and chemical reductions in protein phosphatase activity alter auxin transport, gravity response, and lateral root growth. *Plant Cell* **13**, 1683–1697.
- Raven, J.A. (1975). Transport of indolacetic acid in plant cells in relation to pH and electrical potential gradients, and its significance for polar IAA transport. *New Phytol.* **74**, 163–172.
- Ruegger, M., Dewey, E., Hobbie, L., Brown, D., Bernasconi, P., Turner, J., Muday, G., and Estelle, M. (1997). Reduced naphthylphthalamic acid binding in the *tir3* mutant of *Arabidopsis* is associated with a reduction in polar auxin transport and diverse morphological defects. *Plant Cell* **9**, 745–757.
- Rubery, P.H., and Sheldrake, A.R. (1974). Carrier-mediated auxin transport. *Planta* **118**, 101–121.
- Sabatini, S., Beis, D., Wolkenfelt, H., Murfett, J., Guilfoyle, T., Malamy, J., Benfey, P., Leyser, O., Bechtold, N., Weisbeek, P., and Scheres, B. (1999). An auxin-dependent distal organizer of pattern and polarity in the *Arabidopsis* root. *Cell* **99**, 463–472.
- Sachs, T. (1985). Cellular patterns determined by polar transport. In *Proceedings in Life Science: Plant Growth Substances*, M. Bopp, ed. (New York: Springer Verlag), pp. 231–235.
- Sachs, T. (2000). Integrating cellular and organismic aspects of vascular differentiation. *Plant Cell Physiol.* **41**, 649–656.
- Steeves, T.A., and Sussex, I.M. (1989). *Patterns in Plant Development*. (Cambridge: Cambridge University Press).
- Steinmann, T., Geldner, N., Grebe, M., Mangold, S., Jackson, C.L., Paris, S., Gälweiler, L., Palme, K., and Jürgens, G. (1999). Coordinated polar localization of auxin efflux carrier PIN1 by GNOM ARF GEF. *Science* **286**, 316–318.
- Sundaresan, V., Springer, P., Volpe, T., Haward, S., Jones, J.D., Dean, C., Ma, H., and Martienssen, R. (1995). Patterns of gene action in plant development revealed by enhancer trap and gene trap transposable elements. *Genes Dev.* **14**, 1797–1810.
- Swarup, R., Friml, J., Marchant, A., Ljung, K., Sandberg, G., Palme, K., and Bennett, M. (2001). AUX1 localisation in the *Arabidopsis* root apex reveals two functionally distinct IAA transport pathways. *Genes Dev.* **15**, 2648–2653.
- Teleman, A.A., Strigini, M., and Cohen, S.M. (2001). Shaping morphogen gradients. *Cell* **105**, 559–562.
- Uggla, C., Moritz, T., Sandberg, G., and Sundberg, B. (1996). Auxin as a positional signal in pattern formation in plants. *Proc. Natl. Acad. Sci. USA* **93**, 9282–9286.
- Ulmasov, T., Murfett, J., Hagen, G., and Guilfoyle Tom, J. (1997). Aux/IAA proteins repress expression of reporter genes containing natural and highly active synthetic auxin response elements. *Plant Cell* **9**, 1963–1971.
- Wolpert, L. (1996). One hundred years of positional information. *Trends Genet.* **12**, 359–364.